Dhofar 303, 305, 306, 307, 309, 310, 311, 489, 730, 731, 908, 909, 911, 950, 1085

Anorthositic impact melt breccia

4.15, 34.11, 12.86, 50, 81.3, 10.8, 4, 34.4, 108, 36, 245(9), 3.9, 194(9), 21.7, 197(4) g

Figure 1: Photo of Dhofar 1085 stones as found in the desert location. Black cube is 1 cm.

Introduction

Thirty four individual stones comprise this large and interesting pairing group of impact melt breccias from Oman. Most of these stones lack fusion crust and contain terrestrial weathering products such as gypsum, calcite, celestite, barite, smectite and Fe hydroxides. Exceptions are Dhofar 309 which is partly fusion crusted. Dhofar 303 (Fig. 1) was found in the Dhofar region of Oman (Figs. 2 and 3) in February, 2003. The 4.15 g stone lacks fusion crust, and contains terrestrial weathering products such as calcite, gypsum, celestite, barite, smectite and Fe hydroxides. The circumstances and dates of the finds are too numerous to discuss here, but the interested reader is referred to Russell et al. (2002, 2003, 2004, 2005) for details.

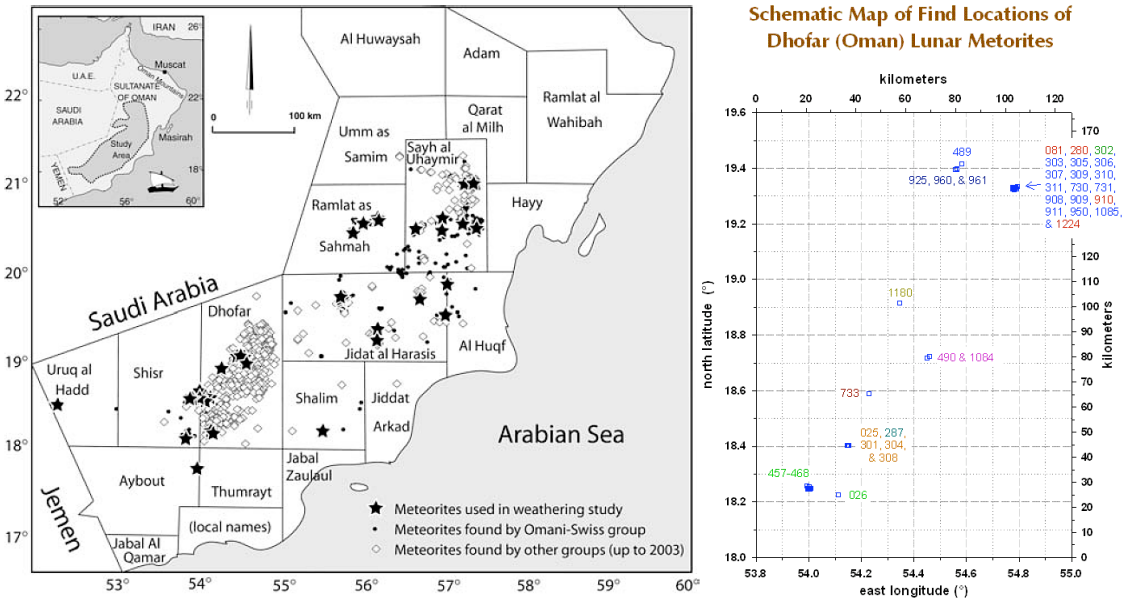

Figure 2 and 3: Location maps of the Dhofar region in Oman (from Al-Kathiri et al., 2005) and the specific coordinates for Dhofar 303, 305, 306, 307, 309, 310, 311, 489, 730, 731, 908, 909, 911, 950, and 1085.

Petrography and mineralogy

This meteorite is an impact melt breccia with mineral and lithic clasts in an impact melt rich matrix (Fig. 4a). The lithic clasts are granulitic, anorthositic, troctolitic, gabbro-noritic, and noritic. A spinel troctolite clast (Fig. 4b) was studied in greater detail by Takeda et al. (2006). Most of the meteorite is comprised of anorthositic or highlands materials, but it is a polymict breccia that also contains mare basalt, KREEP-related materials, and even granitic material (Russell et al., 2004). Diversity within the group is illustrated in Figure 5, where small pieces of Dhofar 303, 305, 306, 309, 911, and 1085 are shown. Accessory minerals in these meteorites are numerous and include ulvospinel, Ti-chromite, pleonaste, ilmenite, silica, troilite, FeNi metal, Ba-bearing potassium feldspar, whitlockite, chlorapatite, baddeleyite, zircon, armalcolite, monazite, tranquillityite, and zirconalite (Russell et al., 2004, 2005).

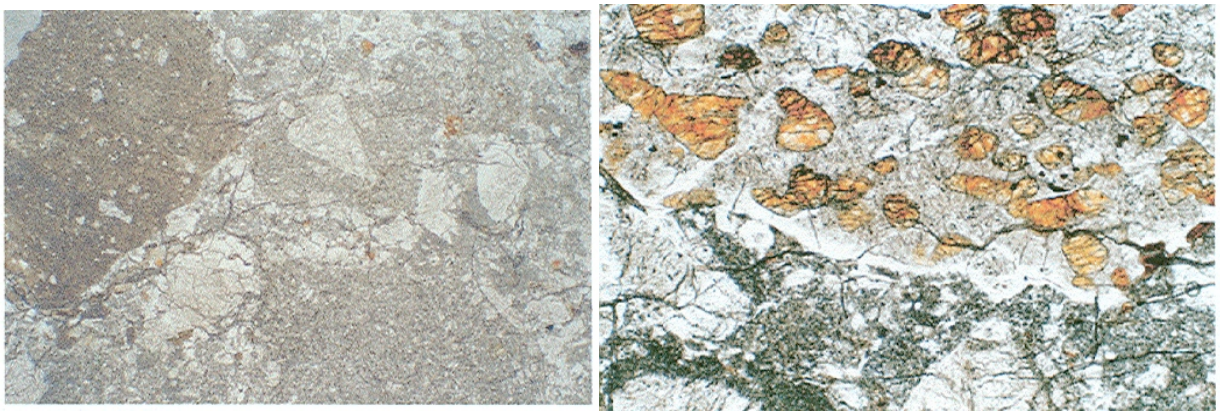

Figure 4a) photomicrograph of a thin section of Dhofar 489 showing the entire view of the crystalline matrix breccia (from Takeda et al., 2003, 2006). Field of view is 6 mm. Figure 4b) photomicrograph of a thin section of the spinel troctolite clast (top half) from Takeda et al. (2004, 2006). Field of view is 3 mm.

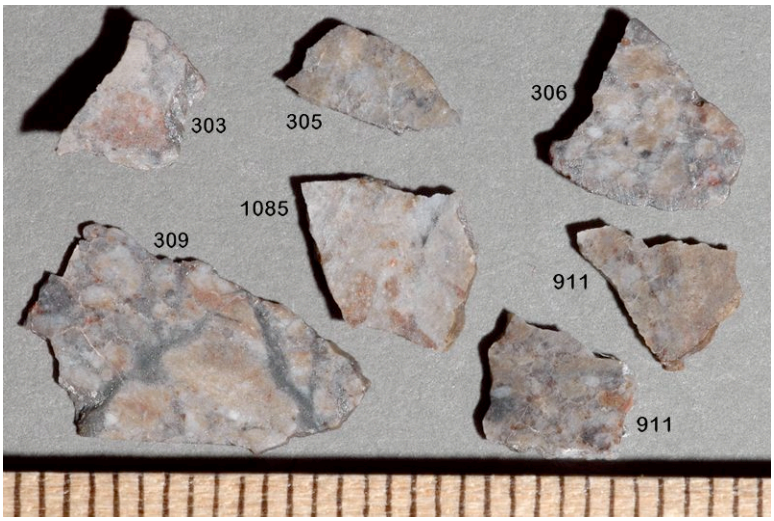

Figure 5: Small pieces of Dhofar 303, 305, 306, 309, 911, and 1085, illustrating the diversity of clast sizes and shapes in this large pairing group (photo from R. Korotev).

The spinel troctolite clasts in Dhofar 489 contain Fo_{85} olivine, but the matrix also contains Fo_{70-77} olivine, suggesting a basaltic influence (Fig. 6). Plagioclase feldspar is An_{94} to $_{98}$ in both the spinel troctolite and the matrix (Fig. 7). Pyroxenes in Dho 489 matrix are similar to those studied in Apollo 16 troctolites, such as those in 60016 (Fig. 8). Overall, olivine, pyroxene, and plagioclase compositions in this Dhofar group are exemplified by intermediate compositions to the field defined by Apollo high Mg suite and ferroan anorthosite (FAN). This is demonstrated well by mineral analyses from Dhofar 304 and 305 (Fig. 9).

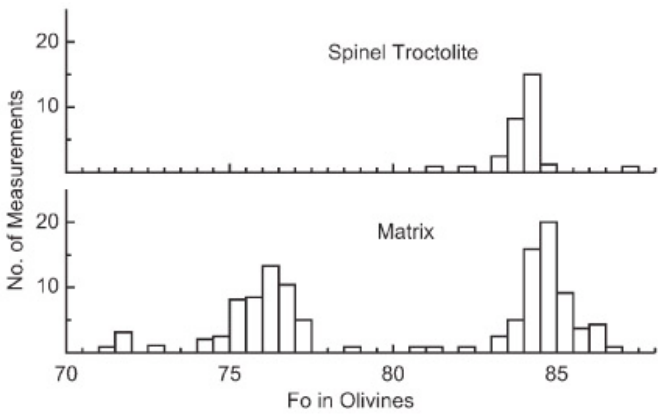

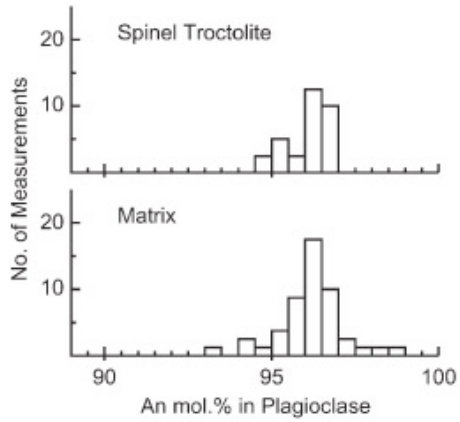

Figure 6: Olivine compositional range in the spinel troctolite and matrix from Dhofar 489 (Takeda et al., 2006). Figure 7: Plagioclase feldspar compositional range in the spinel troctolite and matrix from Dhofar 489 (Takeda et al., 2006).

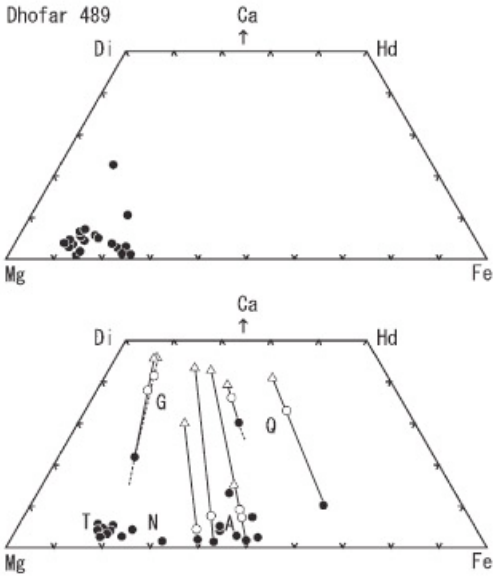

Figure 8: Pyroxene compositions from the matrix of Dhofar 489 (top) compared to those defined by gabbro (G), norite (N), troctolite (T), anorthosite (A) and quartmonzonite (Q) clasts from 60016 (from Takeda et al., 2006).

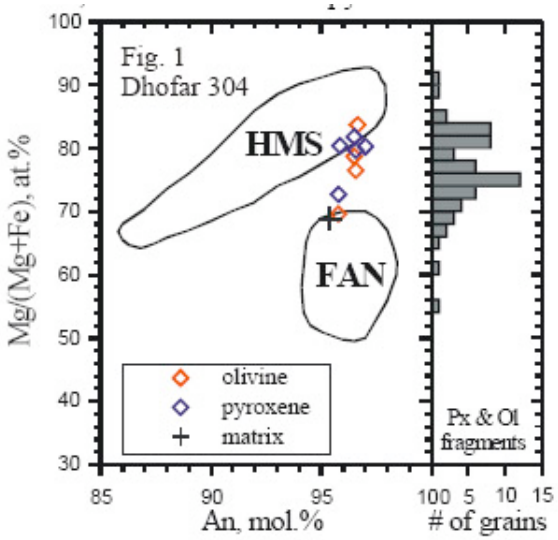

Figure 9: Molar Mg/(Mg+Fe) vs. An content for olivine pyroxene and matrix grains from Dhofar 304 and 305, illustrating their intermediate character between high Mg suite (HMS) and ferroan anorthosite (FAN) clasts from the Apollo collections (from Demidova et al., 2003).

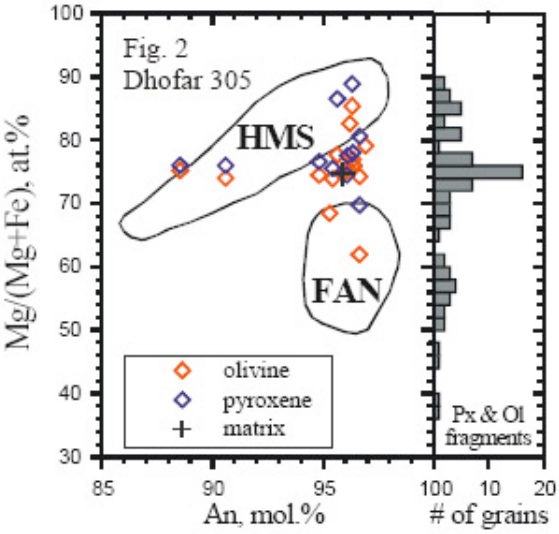

Chemistry

This Dhofar pairing group of meteorites has several unique characteristics (Table 1; note no light or volatile elements have been analyzed for these samples yet), despite the fact that they have typical and low FeO (Fig. 10), and high Al_2O_3 of feldspathic lunar meteorites (Karouji et al., 2004; Korotev, 2006). Thorium contents are lower than most other lunar feldspathic meteorites (Fig. 10). In addition, they have the lowest rare earth element concentrations of any feldspathic meteorites (Fig. 11). Although there are anomalously high U contents, Ba and Sr are also high and the concentrations of all three of these elements could have been enhanced by terrestrial weathering (Korotev, 2006; Nazarov et al., 2004). Miura and Nagao (2004) have measured a solar noble gas component trapped in Dho 489 at high temperatures. These chemical traits (low REE and Th) along with the age information (below) have led some (Takeda et al., 2006) to propose that these meteorites come from the lunar farside where the effects of the Procellarum KREEP Terrane (PKT) and Imbrium basin are absent. Thus, the older age and lower incompatible elements in general. However, Korotev et al. (2006) also point out that some Apollo 16 FANs have equally low Th and Sm, and originate on the near side, and thus a far side origin is not definite (but possible).

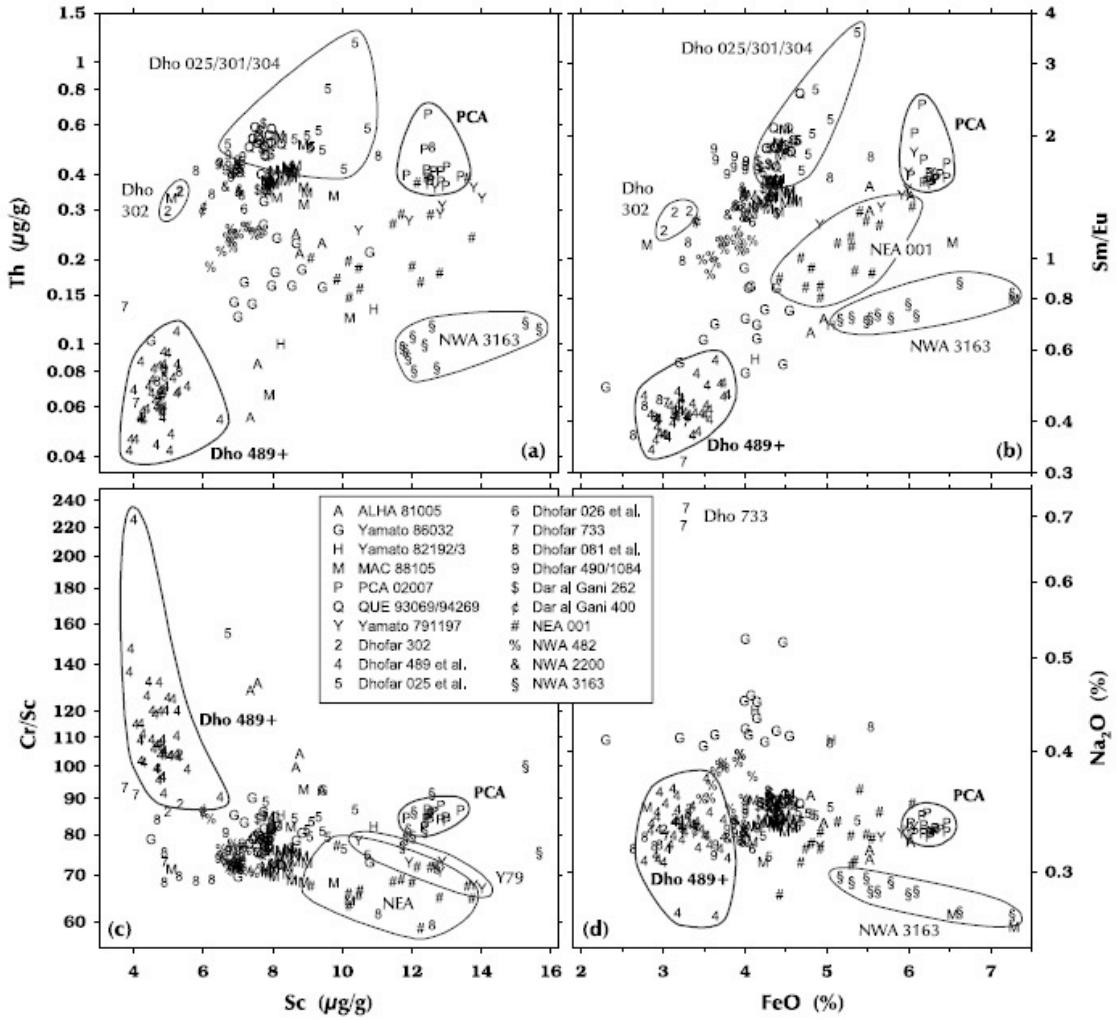

Figure 10: Chemical composition of many paired samples from Dhofar illustrating their low Th, Sm,, Sc and FeO concentrations relative to other feldspathic lunar meteorites (from Korotev et al., 2006).

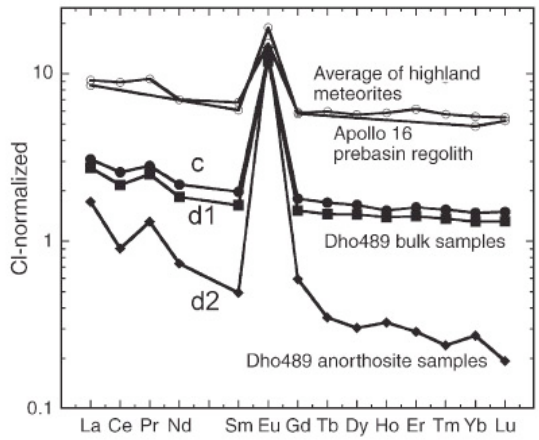

Figure 11: Rare earth element [pattern for Dhofar 489 showing the low concentrations compared to the average of lunar highland meteorites (from Takeda et al., 2006).

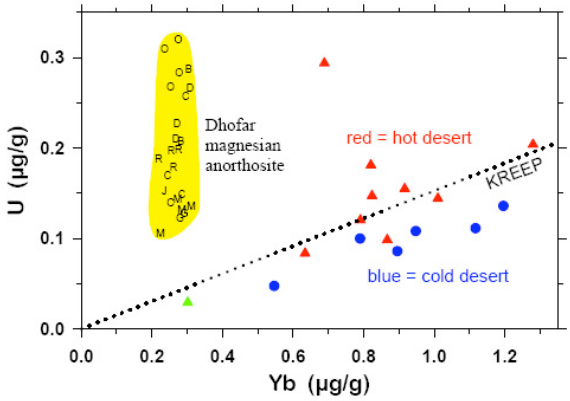

Figure 12:Uranium vs. ytterbium for the Dhofar pairing group (yellow highlighted field) illustrating their unusually high contents relative to other desert lunar highlands meteorites (from Korotev, 2006).

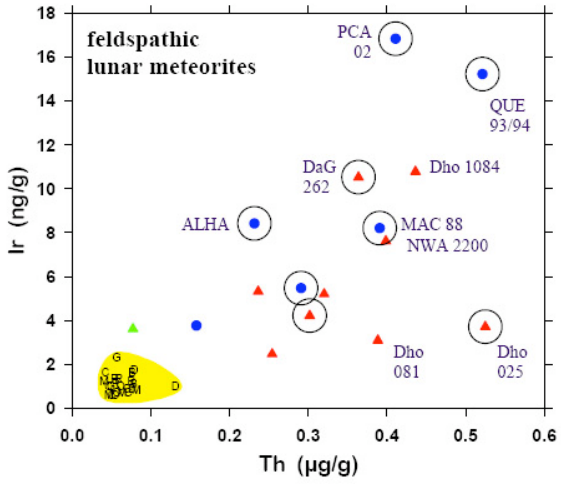

Figure 13: The very low concentrations of the highly siderophile element Ir compared to other feldspathic lunar meteorites (from Korotev, 2006).

Radiogenic age dating

Only ^{39}Ar-^{40}Ar dating has been attempted on this Dhofar group of lunar meteorites (Fernandes et al., 2004; 2006). Whole rock dating of Dho 489 has yielded a plateau age of 4.23 Ga (Takeda et al., 2004, 2006).

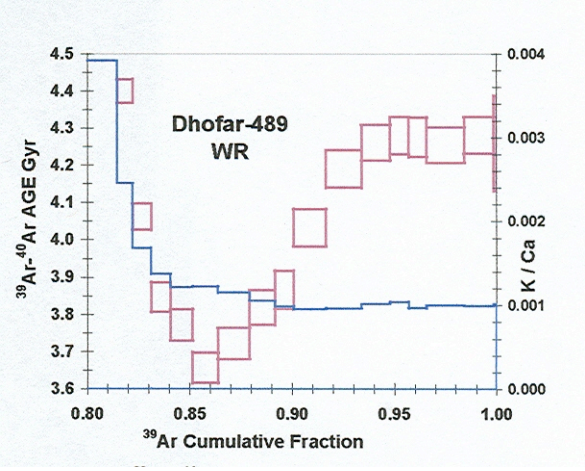

Figure 14: Whole rock dating of Dho 489 has yielded a plateau age of 4.23 Ga (Takeda et al., 2004, 2006).

Cosmogenic isotopes and exposure ages

The low ^{10}Be and ^{4}1Ca measured by Nishiizumi et al. (2004) for several of the paired stones for this group are in agreement with the low fluences measured using Sm and Gd isotopes (Hidaka and Yoneda, 2006). Nishiizumi et al. (2004) propose a 6 +/- 2 kyr transit time for this group.

Table 1: Chemical composition of Dho 489 (paired with 303)

reference	1	1	1	2
weight	143	31	An clast	1200.3
method	b,e,g	b,e,g	b,e,g	d,e
SiO_2 %	43.5	43.9	42.5	43.4
TiO_2	0.104	0.12		0.124
Al_2O_3	27.7	29.8	31.7	27.3
FeO	3.28	2.83	0.46	3.28
MnO	0.0473	0.0376	0.0114	0.056
MgO	6.51	5.58	2.37	7.4
CaO	15.7	17.2	18.5	17.1
Na_2O	0.371	0.36	0.48	0.332
K_2O	0.0361	0.0709		0.021
P_2O_5				0.039
S %				
sum				99.23
Sc ppm				4.74
V				
Cr				540
Co				10.9
Ni				52
Cu				
Zn				
Ga				
Ge				
As				

Se				
Rb				
Sr				700
Y				
Zr				7
Nb				
Mo				
Ru				
Rh				
Pd ppb				
Ag ppb				
Cd ppb				
In ppb				
Sn ppb				
Sb ppb				
Te ppb				
Cs ppm				
Ba				238
La	0.727	0.645	0.405	0.633
Ce	1.56	1.31	0.545	1.60
Pr	0.251	0.224	0.116	
Nd	0.986	0.831	0.333	1.09
Sm	0.291	0.241	0.072	0.301
Eu	0.718	0.668	0.802	0.706
Gd	0.353	0.3	0.117	
Tb	0.0613	0.0525	0.0126	0.067
Dy	0.4	0.351	0.074	
Ho	0.0857	0.0781	0.0184	
Er	0.254	0.225	0.046	
Tm	0.0371	0.0327	0.0057	
Yb	0.241	0.214	0.045	0.273
Lu	0.036	0.0315	0.0046	0.0399
Hf				0.194
Ta				0.029
W ppb				
Re ppb				
Os ppb				
Ir ppb				1.1
Pt ppb				
Au ppb				2.8
Th ppm	0.0634	0.0551	0.0118	0.069
U ppm	0.156	0.143	0.241	0.190

technique (a) ICP-AES, (b) ICP-MS, (c) IDMS, (d) FB-EMPA, (e) INAA, (f) RNAA, (g) PGA
References: 1) Takeda et al. (200); 2) Korotev et al. (2006).